NASA TECHNICAL REPORT

NASA TR R-208

NASA TR R-208

ANALYSIS OF A FREQUENCY TRACKING SQUARE WAVE OSCILLATOR

by R. W. Gunderson

George C. Marshall Space Flight Center
Huntsville, Ala.

NATIONAL AERONAUTICS AND SPACE ADMINISTRATION • WASHINGTON, D. C. • SEPTEMBER 1964

ANALYSIS OF A FREQUENCY TRACKING SQUARE WAVE OSCILLATOR

By R. W. Gunderson

George C. Marshall Space Flight Center
Huntsville, Ala.

NATIONAL AERONAUTICS AND SPACE ADMINISTRATION

For sale by the Office of Technical Services, Department of Commerce,
Washington, D.C. 20230 -- Price $0.75

TABLE OF CONTENTS

LIST OF ILLUSTRATIONS

LIST OF TABLES

DEFINITION OF SYMBOLS

SYMBOL	DEFINITION
$x(t)$	output of integrating element following the x relay
$y(t)$	output of integrating element following the y relay
$I(t)$	the driving square wave function
f_I	frequency of $I(t)$
T_I	period of $I(t)$
$f_{f.r.}$	frequency of output square waves under the free-run condition
$T_{f.r.}$	period of the output square waves under the free-run condition
$f(x)$	output of the x relay section
$f(y)$	output of the y relay section
a	time constant of the integrating elements
x_1	switching level of the x relay
y_1	switching level of the y relay
M	amplitude of the input and relay outputs
t	time
c	M/a
$\Delta\phi$	error in the quadrature phase relationship of the output square waves

ANALYSIS OF A FREQUENCY TRACKING SQUARE WAVE OSCILLATOR

By

R. W. Gunderson

SUMMARY

Presented in this report is an analysis of the lock-on oscillator used as an element in the adaptive tracking notch (ATN) filter currently under development at Marshall Space Flight Center. The analysis is accomplished by studying the phase space behavior of the variables describing operation of the system and permits expressions to be developed through which important properties of the oscillator may be predicted. Examples are given and results of a theoretical study are compared with results obtained from a breadboard mechanization of the system.

SECTION I. INTRODUCTION

The Flight Dynamics Branch of the Astrionics Laboratory has recently designed, built, and tested an adaptive tracking notch (ATN) filter capable of identifying and attenuating very low frequency signals such as those arising from the effect of body bending dynamics in the Saturn class booster vehicles. The basic idea of the ATN filter is to construct a reversed-phase bending signal through modulation techniques and then to sum the constructed signal with the input signal, thereby accomplishing the attenuation. The present configuration has been designed to operate throughout a frequency band of 0.7 to 1.4 Hz, while producing an attenuation of at least 20 to 1 through that range. The ATN filter has no attenuation effect at control mode frequencies and less than 5 degrees of introduced phase lag. A comprehensive discussion on the ATN filter is given in the report by Borelli and Hosenthien (Ref. 1).

The lock-on oscillator is driven by a square wave input of constant amplitude at the bending mode frequency. Its function is to provide two square wave output signals at the same bending frequency but with a 90-degree relative phase shift. Consequently, the unit must be capable of locking onto the input frequency throughout the desired bandwidth and maintaining the quadrature phase relationship of the output signals as an invariant feature.

The analysis was accomplished by studying the phase space behavior of the differential equations describing the system operation. Verification of the analytical results was first obtained through an analog simulation of the system; simulation and analytical results were in close correspondence. A breadboard mechanization of the oscillator was then developed; theoretical results and test results were also in close correspondence.

SECTION II. LOCK-ON OSCILLATOR

The essential features of the unit are shown in Figure 1.

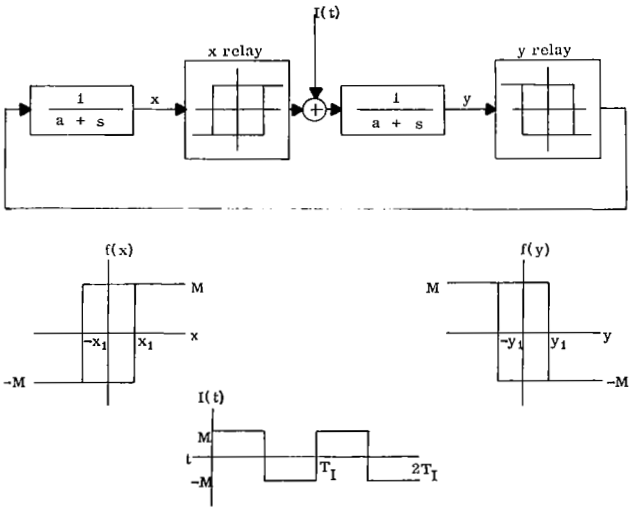

FIGURE 1. BLOCK DIAGRAM OF LOCK-ON OSCILLATOR

The x and y relays are identical except for being of opposite polarity and are assumed to be capable of instantaneous switching action. Switching levels of the relays are denoted by x_1 and y_1 while the output level is denoted by $\pm$ M. The absolute value of the input, I(t), is the same as the absolute value of the relay outputs; that is, $|I(t)| = M$. For purposes of the analog simulation, the nonlinear characteristic of the x and y relays was obtained through the use of nonlinear, high gain feedback methods as given in a paper by Terrazas and Fannin (Ref. 2). The circuitry allowed a great deal of versatility coupled with a precise simulation of the desired nonlinearity.

SECTION III. FREE-RUNNING CASE, $I(t) \equiv 0$

The behavior of the system will first be studied in its free-running condition; that is, with the input $I(t) \equiv 0$ for all $t \geq 0$. By studying the behavior of the trajectories in the two-dimensional phase space of the variables x and y, an insight will be gained into system operation and an equation for the period of the limit cycle will be derived.

Assume that the values $f(x)$ and $f(y)$ remain constant during the time interval $t_1 \geq t > t_0$. Since $I(t) \equiv 0$, the differential equations describing the operation of the system during that interval are written as

$$\frac{d\,x(t)}{dt} + ax(t) = f(y)$$
$$\frac{d\,y(t)}{dt} + ay(t) = f(x) \quad . \tag{1}$$

The solutions of the two equations, valid during $t_1 \geq t > t_0$, are obtained in the form

$$x(t) = \frac{f(y)}{a} + e^{-a(t-t_0)}\left[x(t_0) - \frac{f(y)}{a}\right]$$
$$y(t) = \frac{f(x)}{a} + e^{-a(t-t_0)}\left[y(t_0) - \frac{f(x)}{a}\right]. \qquad (t_0 < t \leq t_1) \tag{2}$$

The differential equations (1) provide the differential equation of the trajectories as

$$\frac{d\,y(t)}{d\,x(t)} = \frac{f(x) - ay(t)}{f(y) - ax(t)} \quad . \tag{3}$$

From equation (3), it is apparent that the system will have a singular point, or equilibrium, at the point of the x-y space given by

$$x = \frac{f(y)}{a} \quad , \quad y = \frac{f(x)}{a} \quad . \tag{4}$$

The trajectory will then originate at the point $(x(t_0), y(t_0))$ and tend toward the singularity determined by equation (4) along the straight line

$$\frac{x - \frac{f(y)}{a}}{y - \frac{f(x)}{a}} = \frac{x(t_0) - \frac{f(y)}{a}}{y(t_0) - \frac{f(x)}{a}} \qquad (t_0 < t \leq t_1) \tag{5}$$

as given by the solution of equation (3). If at time $t = t_1$ either $f(x)$ or $f(y)$ should change polarity, the system will enter a new mode of operation. Here the initial conditions are the final values $(x(t_1), y(t_1))$ of the preceding mode and the singularity will change with equation (4). In this manner, it is possible to follow the system through its succeeding modes of operation.

For example, assume that the system begins operation at time $t = 0$ and is such that $x(0) = y(0) = 0$ while the output of both relays is initially negative. The trajectory will initially try to reach a singularity at the point $(-M/a, -M/a)$ and will tend toward that point on the straight line given by equation (5), as shown in Figure 2. However, when the trajectory intersects the switching line $y = -y_1$, the y relay will switch polarity to +M and the trajectory will tend toward a new singularity at $(M/a, -M/a)$. When the trajectory intersects the switching line $x = x_1$, the system will again assume a new singularity at $(M/a, M/a)$ and so on.

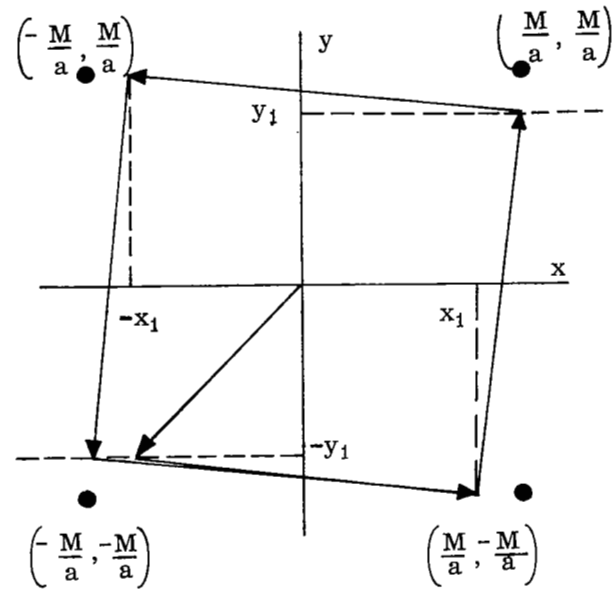

FIGURE 2. TYPICAL FREE-RUNNING TRAJECTORY

SECTION IV. LIMIT CYCLE

As shown by Figure 2, the trajectory soon converges to a closed curve about the origin; that is, the system possesses a stable limit cycle. To determine exactly the path of the limit cycle, it is necessary only to calculate one point on that curve, since knowledge of that point and the singularities allows construction of the rest of the curve. Consequently, let $x(t_0)$ be some point along the switching line $y = y_1$ and let $f(x)$ and $f(y)$ have the values M and -M, respectively. From equation (5) the equation of the first straight line segment of the trajectory is then

$$\frac{y - c}{x + c} = \frac{y_1 - c}{x(t_0) + c} \tag{6}$$

where

$$c = \frac{M}{a} \quad .$$

The trajectory will tend toward the singularity at $(-M/a, M/a)$ but will intersect the $-x_1$ switching line at some time $t = t_1$. At time t_1, the system begins a new mode of operation and tries to reach the singularity at $(-M/a, -M/a)$. Taking into account the symmetry of trajectory behavior, if the trajectory intersects the $-y_1$ switching line at the point $-x(t_0)$, then the trajectory is the curve of the limit cycle.

At $t = t_1$, equation (6) becomes

$$y - c = \frac{-(x_1 - c)\,(y_1 - c)}{(x(t_0) + c)} . \tag{7}$$

Accordingly, the initial conditions for the second operation mode are

$$x = -x_1, \; y = \frac{-(x_1 - c)\,(y_1 - c) + c(x(t_0) + c)}{(x(t_0) + c)} \tag{8}$$

and the equation of the trajectory becomes

$$\frac{y + c}{x + c} = \frac{-(x_1 - c)\,(y_1 - c) + 2c(x(t_0) + c)}{-(x(t_0) + c)\,(x_1 - c)} \tag{9}$$

for $t \geq t_1$. This part of the trajectory intersects the $y = -y_1$ switching line. As previously explained, if it is to be the equation of the limit cycle, it must be that $x(t_2) = -x(t_0)$ where t_2 is the time of intersection with the $-y_1$ switching line. That is,

$$x(t_2) + c = -x(t_0) + c = \frac{(y_1 - c)\,(x_1 - c)\,(x(t_0) + c)}{2c(x(t_0) + c) - (x_1 - c)\,(y_1 - c)}$$

and solving for $x(t_0)$ yields

$$x(t_0) = \sqrt{c(x_1 + y_1) - x_1 y_1} \quad . \tag{10}$$

The period of the limit cycle can now be derived by using the initial conditions as calculated above. To do so, symmetry considerations show it is necessary to solve only for the time required to travel from the calculated point $(x(t_0), y_1)$ to $(-x_1, y_1)$, since this furnishes the time of the quarter-period.

From equation (2) and equation (10)

$$-x_1 = -c + e^{-at}\left[\sqrt{c(x_1 + y_1) - x_1 y_1} + c\right]$$

$$at = \ell n \left[\frac{c + \sqrt{c(x_1 + y_1) - x_1 y_1}}{c - x_1}\right],$$

so that the complete period of the limit cycle is obtained as

$$T_{f.r.} = \frac{4}{a} \ell n \left[\frac{c + \sqrt{c(x_1 + y_1) - x_1 y_1}}{c - x_1}\right]. \tag{11}$$

SECTION V. DRIVEN CONDITION

The ATN filter concept presently requires the lock-on oscillator to be driven by a square wave input signal at the bending frequency when the amplitude of the bending signal exceeds a certain preset value. When operating under the driven condition, it is required that the system produce two symmetrical square wave outputs, $f(x)$ and $f(y)$, which are to be at the bending frequency with a quadrature phase relationship. Since the bending mode frequencies vary as a function of time of flight, the oscillator must follow the frequency of the input throughout the expected range of variation with the property of the quadrature phase relationship kept essentially invariant.

Consider the system during a time interval $t_0 < t \leq t_1$ for which the values of $f(x)$, $f(y)$, and $I(t)$ are constant. The differential equations describing the operation during that interval are

$$\frac{d\,x(t)}{dt} + a x(t) = f(y)$$

$$\frac{d\,y(t)}{dt} + a y(t) = f(x) + I(t) \quad . \tag{12}$$

The equations for $x(t)$ and $y(t)$, valid during $t_0 < t \leq t_1$, are obtained from equation (12) as

$$x(t) = \frac{f(y)}{a} + e^{-a(t-t_0)}\left[x(t_0) - \frac{f(y)}{a}\right] \tag{13}$$

$$y(t) = \frac{f(x) + I(t)}{a} + e^{-a(t-t_0)}\left[y(t_0) - \frac{f(x) + I(t)}{a}\right]$$

and the differential equation of the trajectory becomes

$$\frac{dy}{dx} = \frac{f(x) + I(t) - ay}{f(y) - ax} \quad . \tag{14}$$

Equation (14) determines the location of the singularity as

$$x = \frac{f(y)}{a}, \quad y = \frac{f(x) + I(t)}{a}, \tag{15}$$

where, since $f(x)$, $f(y)$, and $I(t)$ all have the same magnitude but can differ in polarity, there are now the six possible singularities shown in Figure 3.

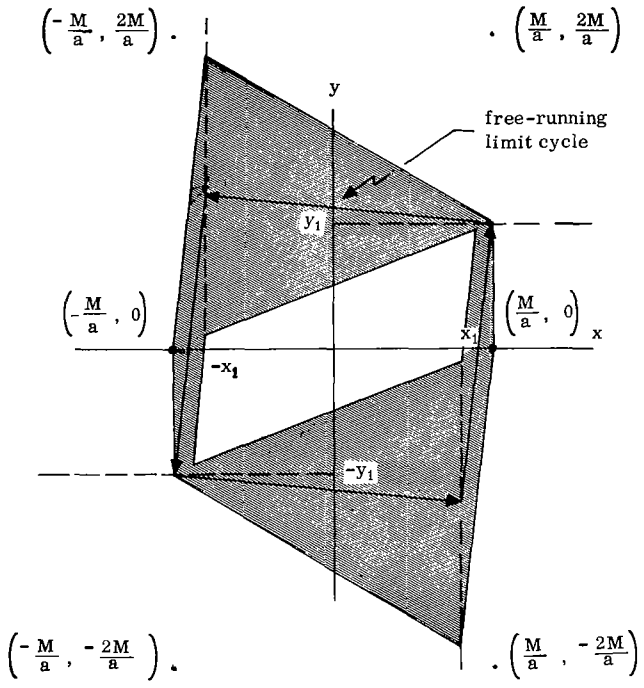

FIGURE 3. SINGULARITIES FOR THE DRIVEN CASE AND BOUNDS FOR THE TRAJECTORY

Generally, the phase space study of system behavior is considerably complicated by the introduction of a time dependent driving function. For example, in the undriven case, if the trajectory intersects a switching line at a point (x_1, y_1), then the trajectory must continue along the straight line drawn from that point to the singularity in the following quadrant. That is, a unique segment of the trajectory originates from each point on a switching line and this segment can be determined simply by knowledge of singularity locations. However, in the driven case, an infinite number of possible paths for the trajectory exist for each point on a switching line. Such a circumstance results from the presence of the I(t) term, a time dependent function, in the expression for the singularities given by equation (15). On the other hand, particularly since I(t) is a square wave function with known period and amplitude, the phase space approach still provides a comparatively convenient method for answering the required questions on oscillator behavior.

Consider first the shaded region of the phase space shown in Figure 3. Under the system design philosophy, the lock-on oscillator will always be in its free-running condition before an input signal is applied. Consequently, the trajectories to be considered will both begin and remain in a region such as that shown in Figure 3. The boundary of the region is constructed simply by considering the extreme possibilities of trajectory behavior. For example, trajectories originating at the point $(M/a, y_1)$ will initially tend toward the singularities

$$x = -\frac{M}{a}\ , \quad y = \frac{M}{a} \pm \frac{M}{a}\ .$$

The two extreme possibilities are thus the straight lines continued toward the singularities until intersection with the $-x_1$ switching lines.

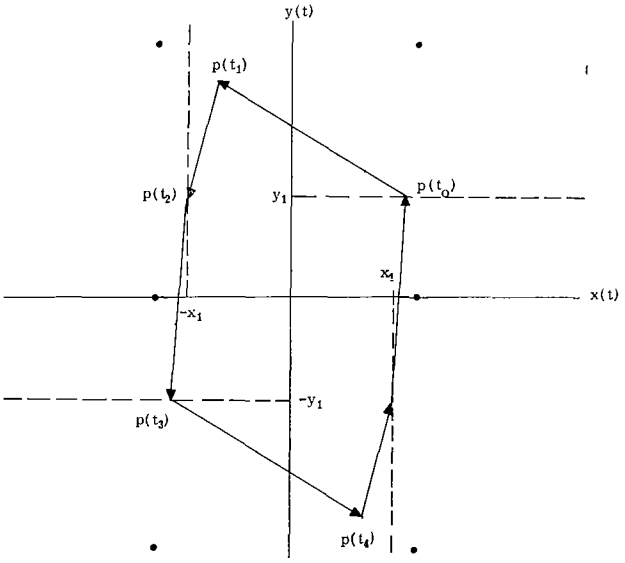

FIGURE 4. PERIODIC TRAJECTORY FOR THE DRIVEN CASE

Now consider the closed trajectory of Figure 4. In addition to the four switching points caused by intersection of the curve with the x and y switching lines, it is now necessary to locate the switching points caused by a change of polarity in the driving signal, I(t). During the time interval $t_0 < t \leq t_1$ when the trajectory is traveling between points $p(t_0)$ and $p(t_1)$, the equations of the x and y motions are given by

$$x(t) = -\frac{M}{a} + e^{-a(t-t_0)}\left[x(t_0) + \frac{M}{a}\right]$$

and $(t_0 < t \leq t_1)$

$$y(t) = 2\frac{M}{a} + e^{-a(t-t_0)}\left[y(t_0 - 2\frac{M}{a}\right] .$$

At $t = t_1$ the polarity of I(t) changes from + M to - M so that the equation of the y motion during the interval $t_1 < t \leq t_2$ is changed to

$$y(t) = e^{-a(t-t_1)}\, y(t_1)\ , \qquad (t_1 < t \leq t_2)$$

while the x motion is unchanged. The trajectory continues in like manner until $T_I/2$ seconds after the change of polarity at $p(t_1)$, when the input once again changes sign. If now

$$p(t_4) = (x(t_1 + T_I/2),\ y(t_1 + T_I/2)) =$$

$$= (-x(t_1),\ -y(t_1)) = -p(t_1),$$

then, as time continues, the trajectory must return to the starting point $p(t_0)$ so that

$$(x(t_0 + T_I),\ y(t_0 + T_I)) = (x(t_0),\ y(t_0)).$$

Consequently, the trajectory will be periodic in T_I and symmetrical; that is,

$$x(t + T_I/2) = -x(t)$$

$$y(t + T_I/2) = -y(t)\ .$$

With the exception of quadrature phase relationship between f(x) and f(y), a periodic trajectory such as that of Figure 4 describes the desired operation of the lock-on oscillator. The quadrature phase relationship will be obtained only if

$$t_2 - t_0 = t_3 - t_2.$$

Figure 5 shows the input and output square waves corresponding to the trajectory of Figure 4.

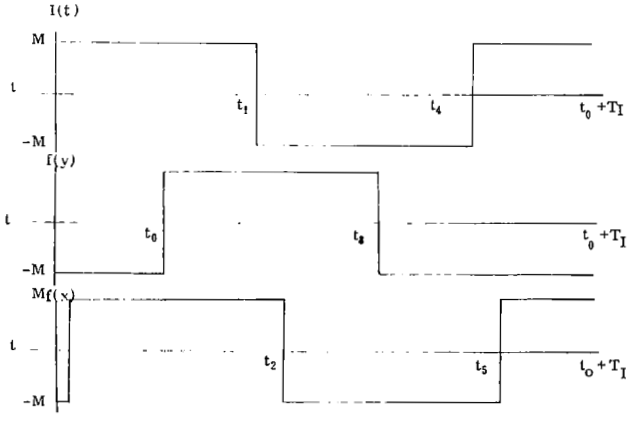

FIGURE 5. INPUT AND OUTPUT SQUARE WAVES CORRESPONDING TO THE PERIODIC TRAJECTORY OF FIGURE 4

Notice that the x motion is independent of I(t). Hence it is possible to solve for the value of x(t) at the instant the y relay switches to its negative polarity and such that, after $T_I/2$ seconds later, x(t) will be at the negative of this value. That is, it is possible to solve for the x(t) values at the instant of y relay switching necessary to maintain the periodic trajectory. This value is obtained from equation (13) as

$$x_0 = \frac{M}{a}\left[\frac{1 - e^{-a\,T_I/2}}{1 + e^{-a\,T_I/2}}\right] = c \tanh \frac{a\,T_I}{4}, \qquad (16)$$

where x_0 denotes the desired value.

If the period of the input square wave I(t) is known, x_0 can be calculated from equation (16) and the periodic trajectory can be constructed as illustrated by Figure 6 (a and b). The procedure is to draw first a straight line through the point $(-x_0, -y_1)$ and the singularity in the third quadrant; then a straight line through (x_0, y_1) and the singularity in the second quadrant. If the two lines intersect to the left of the $-x_1$ switching line, the two segments are connected as shown in Figure 6(a). If they intersect to the right of the $-x_1$ line, then the segments are connected as shown in Figure 6(b).

Equation (16) indicates x_0 will decrease with the period of the driving signal. Consequently the area enclosed by the periodic trajectories indicating satisfactory behavior must decrease as the frequency of the driving signal increases. However, as illustrated by Figure 3, there is a lower limit to the enclosed area. That is, the closed trajectories indicating satisfactory behavior can exist only for a finite frequency range of the input square wave. It is possible to write an analytic expression for determining the frequency range; however, it would seem more convenient to do so through a phase space construction procedure. First, notice from Figure 6(b) that the "smallest" trajectory corresponds to the case when the y relay and I(t) polarity changes occur simultaneously. That is, the segment of the trajectory lying on the straight line through (x_0, y_1) and the singularity in the second quadrant approaches zero length. Begin the trajectory at the point (x_1, y_1), as shown in Figure 7, and continue towards the appropriate singularities. By assuming the I(t) polarity changes occur at the instant of y relay switching, it is found that the curve soon converges to the desired smallest periodic trajectory.

The period, T_I, corresponding to the value of x_0 determined can then be obtained through equation (16). It can be seen from equation (16) and Figure 6(a) that there is no lower positive limit to the frequency permitting periodic behavior. Consequently the desired periodic trajectories exist for a frequency band extending from arbitrarily near zero to the value determined through the procedure previously given.

To this point, it has been established that there exist only periodic trajectories indicating satisfactory behavior of the lock-on oscillator. Equation (16) is only a special case of the more general expression

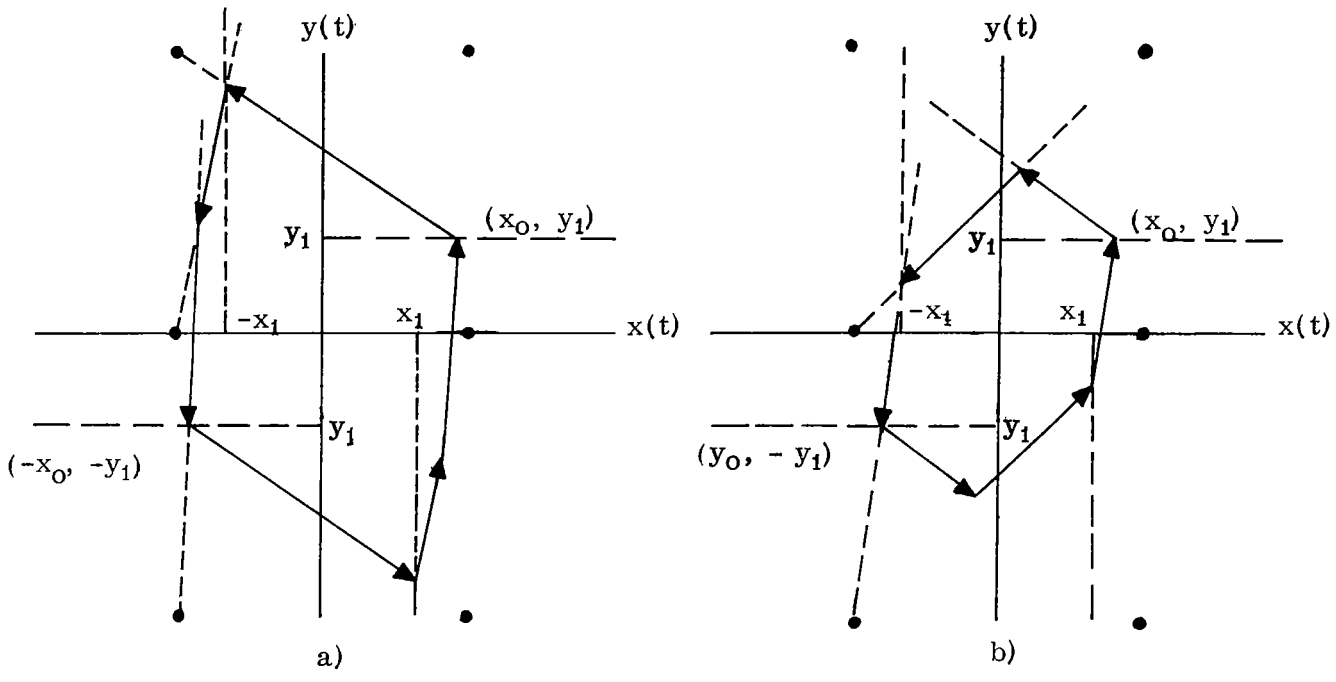

FIGURE 6. CONSTRUCTION OF PERIODIC TRAJECTORIES FOR KNOWN VALUES OF x_0

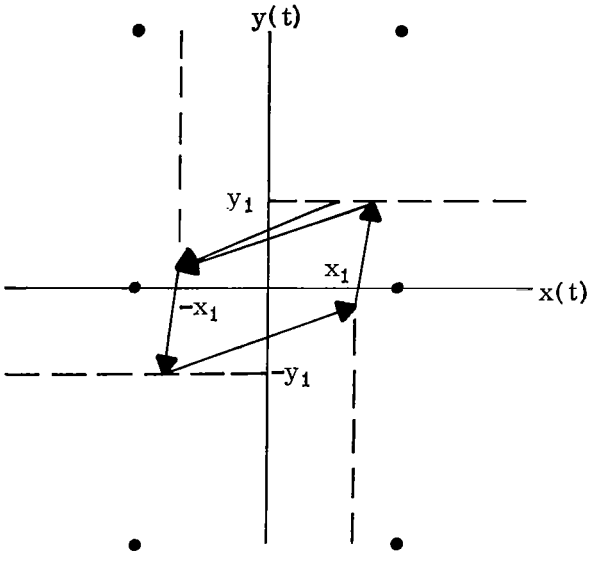

FIGURE 7. CONSTRUCTION OF SMALLEST PERIODIC TRAJECTORY

$$x_0 = \frac{M}{a}\left[\frac{1 - e^{-ak\,T_I/2}}{1 + e^{-ak\,T_I/2}}\right] = c\tanh\frac{ak\,T_I}{4} \qquad (17)$$

$(k = 1, 2, 3, \ldots)$

which provides the value of x(t) at the instant of y relay switching necessary to maintain periodic trajectories describing subharmonic tracking of the system. That is, between switching of the relays from one polarity to the opposite, the input will have changed polarity k times. The following discussion will show that such trajectories do exist, but only for odd values of k.

The closed trajectories of Figure 8 typify the two types of trajectories which can exist for k = 3. To solve for the time $t_1 - t_0$ of Figure 8(a), begin with the y(t) motion at $t = t_0$ and continue until $t = t_5$ to obtain

$$\begin{aligned}
y(t_1) &= 2c + e^{-a(t_1 - t_0)} \quad [y_1 - 2c] \quad (t_0 < t \le t_1)\\
y(t_2) &= e^{-a(t_2 - t_1)}\, y(t_1) \quad (t_1 < t \le t_2)\\
y(t_3) &= -2c + e^{-a(t_3 - t_2)} \quad [y(t_2) + 2c] \quad (t_2 < t \le t_3)\\
y(t_4) &= e^{-a(t_4 - t_3)}\, y(t_3) \quad (t_3 < t \le t_4)\\
y(t_5) &= -2c + e^{-a(t_5 - t_4)} \quad [y(t_4) + 2c] \quad (t_4 < t \le t_5)
\end{aligned} \qquad (18)$$

and conbine to obtain

$$\begin{aligned}
y(t_5) = {} & -2c + 2ce^{-a(t_5 - t_4)} - 2ce^{-a(t_5 - t_3)}\\
& + 2ce^{-a(t_5 - t_2)} + 2ce^{-a(t_5 - t_1)}\\
& + e^{-a(t_5 - t_0)}\,(y_1 - 2c).
\end{aligned} \qquad (19)$$

Since

$$e^{-a(t_5 - t_4)} = e^{-a\,T_I/2}\, e^{a(t_1 - t_0)}$$

$$e^{-a(t_5 - t_3)} = e^{-a\,T_I}\, e^{a(t_1 - t_0)}$$

$$e^{-a(t_5 - t_2)} = \frac{c + x(t_5)}{c - x_1} \qquad (20)$$

$$e^{-a(t_5 - t_1)} = e^{-3a\,T_I/2}\, e^{a(t_1 - t_0)}$$

$$e^{-a(t_5 - t_0)} = e^{-3a\,T_I/2},$$

substitution into equation (19) yields

$$e^{a(t_1 - t_0)} = \frac{\left(1 - \frac{y_1}{2c}\right)\left(1 + e^{-3a/2\,T_I}\right) - \frac{c + x(t_5)}{c - x_1}}{e^{-a/2\,T_I}\left(1 - e^{-a\,T_I/2} + e^{-a\,T_I}\right)} \qquad (21)$$

and since

$$e^{-a(t_1 - t_0)} > e^{-a/2\,T_I},$$

the inequality

$$\frac{1 - e^{-a\,T_I/2} + e^{-a\,T_I}}{(1 - y_1/2c)\left(1 + e^{-3a/2\,T_I}\right) - \frac{c + x(t_5)}{c - x_1}} > 1 \qquad (22)$$

must then be satisfied. Let

$$s = e^{-a/2\,T_I}$$

so that from

$$c + x(t_5) = c - c\left(\frac{1 - e^{-3a/2\,T_I}}{1 + e^{-3a/2\,T_I}}\right) =$$

$$= \frac{2ce^{-3a/2\,T_I}}{\left(1 + e^{-3a/2\,T_I}\right)}$$

and from equation (22),

$$\frac{1 - s + s^2}{\left(1 - \frac{y_1}{2c}\right)(1 + s^3) - \frac{2s^3}{(1 + s^3)\left(1 - \frac{x_1}{c}\right)}} > 1$$

or

$$\left(1 - \frac{x_1}{c}\right)(1 - s + s^2)(1 + s^3) > \qquad (23)$$

$$> \left(1 - \frac{x_1}{c}\right)\left(1 - \frac{y_1}{2c}\right)(1 + s^3)^2 - 2s^3.$$

For the moment, assume

$$\frac{x_1}{c} \to 0$$

$$\frac{y_1}{2c} \to 0$$

so that inequality (23) becomes

$$s(-s^5 + s^4 - s^3 + s^2 + s - 1) > 0$$

or

$$s(1 - s)\left(s^2 + \frac{1 + \sqrt{5}}{2}\right)\left(s^2 + \frac{1 - \sqrt{5}}{2}\right) > 0. \qquad (24)$$

Consequently under the assumption that x_1/c and $x_1/2c$ are sufficiently small, inequality (22) is satisfied if

$$1 > s > \sqrt{\frac{\sqrt{5} - 1}{2}}$$

that is,

$$T_I < \frac{2}{a}\,\ell n\left[\sqrt{\frac{2}{\sqrt{5} - 1}}\right]. \qquad (25)$$

Rewriting equation (23) in the form

$$(1 - s + s^2)(1 + s^3) > (1 - y_1/2c)(1 + s^3)^2 \qquad (26)$$

$$- \frac{2s^3}{\left(1 - \frac{x_1}{c}\right)}$$

and noting that

$$(1 + s^3)^2 - 2s^3 > \left(1 - \frac{y_1}{2c}\right)(1 + s^3)^2 - \frac{2s^3}{\left(1 - \frac{x_1}{c}\right)}$$

(for $y_1 > 0$, $x_1 > 0$, $\frac{x_1}{c} < 1$) shows that inequality (25) provides the greatest value, T_I, for which closed trajectories corresponding to $k = 3$, and of the form shown in Figure 8(a), always exist. Given values for x_1, y_1, and c, the corresponding maximum value of T_I can be obtained by factoring equation (23) in the manner shown for the particular case of $x_1 = y_1 = 0$.

Now consider Figure 8(b) and start again at $t = t_0$ to obtain

$$y(t_1) = 2c + e^{-a(t_1 - t_0)}\,[y_1 - 2c] \quad (t_0 < t \leq t_1) \qquad (27)$$

$$y(t_2) = e^{-a(t_2 - t_1)}\, y(t_1) \qquad (t_0 < t \le t_2)$$

$$y(t_3) = 2c + e^{-a(t_3 - t_2)}\,[y(t_2) - 2c] \quad (t_2 < t \le t_3)$$

$$y(t_4) = e^{-a(t_4 - t_3)}\, y(t_3) \qquad (t_3 < t \le t_4) \tag{27}$$

$$y(t_5) = -2c + e^{-a(t_5 - t_4)}\,[y(t_4) + 2c] \quad (t_4 < t \le t_5)$$

and

$$e^{-a(t_5 - t_4)} = e^{-a\,T_I/2}\, e^{a(t_1 - t_0)}$$

$$e^{-a(t_5 - t_3)} = \frac{c + x(t_5)}{c - x_1}$$

$$e^{-a(t_5 - t_2)} = e^{-a\,T_I}\, e^{a(t_1 - t_0)} \tag{28}$$

$$e^{-a(t_5 - t_1)} = e^{-a3\,T_I/2}\, e^{a(t_1 - t_0)}$$

$$e^{-a(t_5 - t_0)} = e^{-3a/2\,T_I}\,.$$

Substituting equation (28) into equation (27), combining, and solving for $e^{a(t_1 - t_0)}$ then yield

$$e^{a(t_1 - t_0)} = \frac{(1 - y_1/2c)\left(1 + e^{-3a\,T_I/2}\right) - \frac{c + x(t_5)}{c - x_1}}{e^{-a\,T_I/2}\,(1 - e^{-a\,T_I/2} + e^{-a\,T_I})} \tag{29}$$

which is identical with equation (21). Consequently the results obtained for Figure 8(a) also hold for Figure 8(b).

Notice now that the trajectory can intersect the positive y_1 switching line only if the input signal polarity is positive and can intersect the negative y_1 switching line only if the input polarity is negative. Consequently the polarity of the input can only change an odd number of times between positive and negative switching of the y relay. That is, k of equation (17) must be odd.

Figure 9 illustrates the trajectory of next highest order, k = 5. The expression corresponding to equation (21) is obtained in the same manner for k = 5 and is of the form

$$e^{a(t_1 - t_0)} = \tag{30}$$

$$\frac{(1 - y_1/2c)\,(1 + e^{-5a/2\,T_I}) - \frac{c + x(t_7)}{c - x_1}}{e^{-aT_I/2}\,(1 - e^{-aT_I/2} + e^{-aT_I} - e^{-3aT_I/2} + e^{-2aT_I})}\,.$$

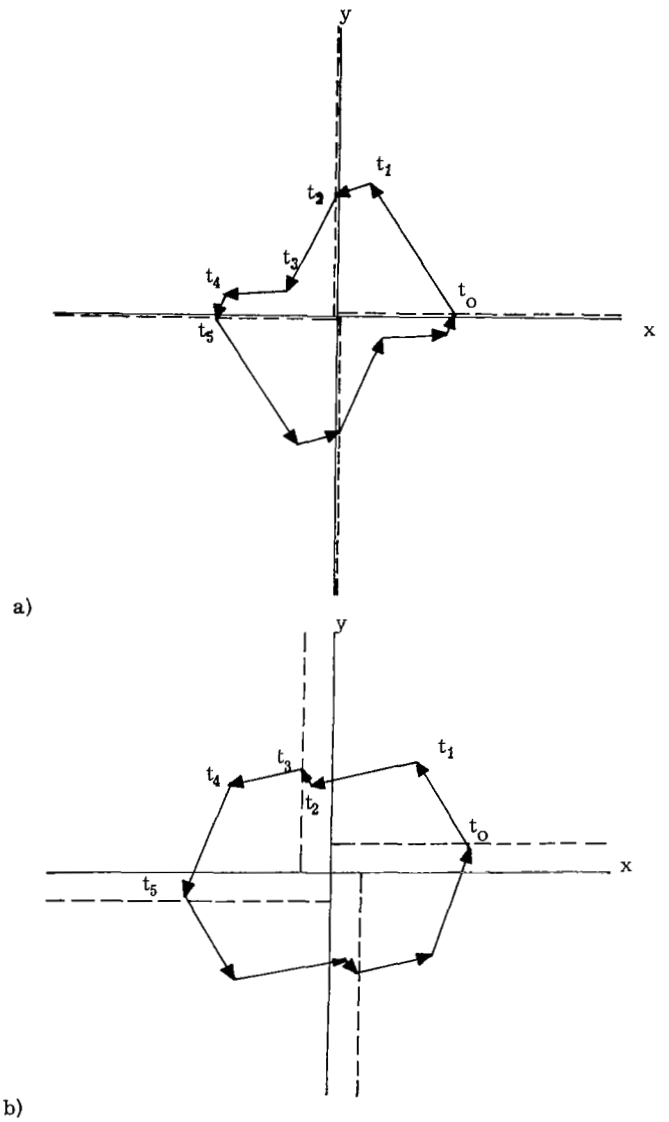

FIGURE 8. PERIODIC TRAJECTORIES CORRESPONDING TO k = 3

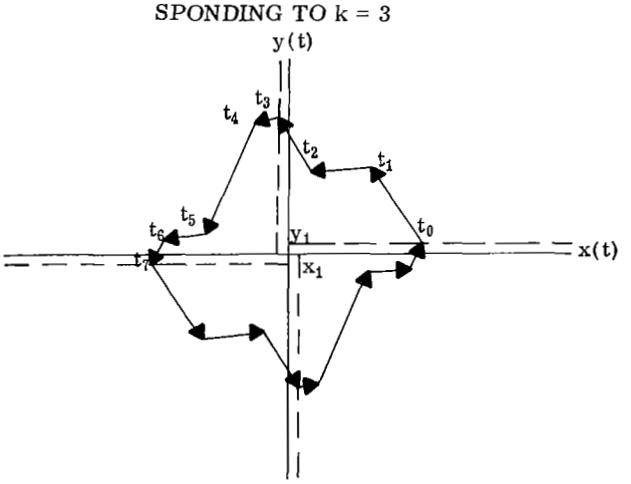

FIGURE 9. PERIODIC TRAJECTORY CORRESPONDING TO k = 5

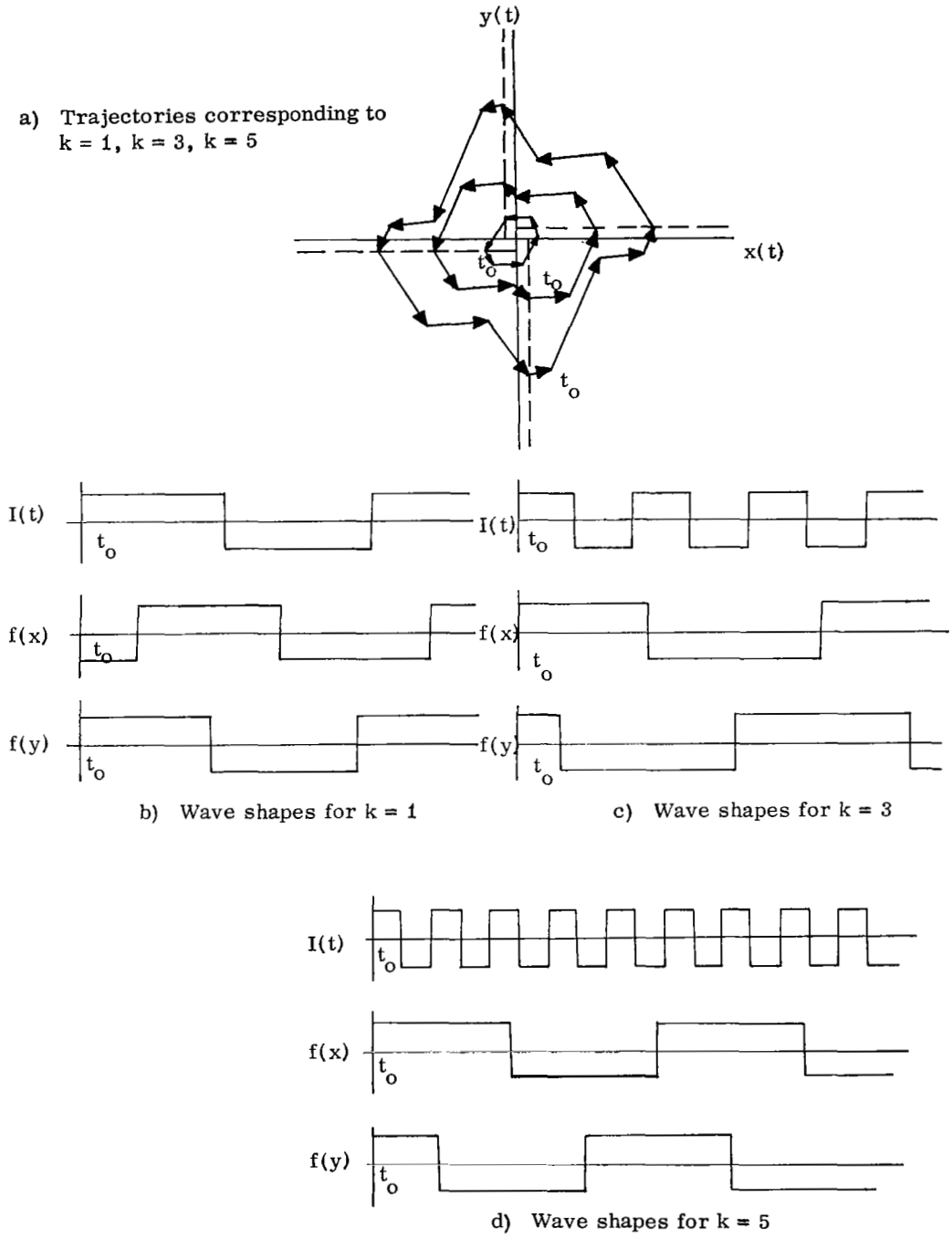

FIGURE 10. THREE POSSIBLE PERIODIC MODES OF OPERATION

Again assume that $y_1/2c \to 0$, $x_1/c \to 0$ and let $s = e^{-a\,T_I/2}$. The inequality corresponding to equation (24) is of the form

$$s(1 - s)(s^8 + s^6 + s^4 - s^2 - 1) > 0. \qquad (31)$$

Rewriting this inequality as

$$s(1 - s)[s^2(s^4 + s^2 - 1) + (s^8 - 1)] > 0$$

and noting that the expression in brackets is positive for $s = 1$ but negative for $s^2 = \frac{\sqrt{5}-1}{2}$ indicates that polynomial of equation (31) possesses a zero, h, such that

$$s > h > \sqrt{\frac{\sqrt{5}-1}{2}}$$

must be true before inequality (31) is satisfied. That is,

$$T_I < \frac{2}{a}\,\ell n\, h^{-1} < \frac{2}{a}\,\ell n \sqrt{\frac{2}{\sqrt{5}-1}}\ . \qquad (32)$$

Figure 10 is a typical case of a system for which trajectories corresponding to k = 1, k = 3, and k = 5 exist for a given frequency. The time response is shown for each case.

The discussion above shows that the lowest frequency of the driving signal necessary to maintain a k = 5 trajectory must be greater than the lowest frequency necessary for a trajectory of k = 3. In exactly the same manner, trajectories corresponding to k values greater than 5 can be shown to exist only for input signal frequencies which satisfy inequality (32). Inasmuch as the particular application of the lock-on oscillator being considered here requires tracking through a frequency range of 0.7 to 1.4 Hz (page 1), no difficulty with subharmonic lock-on operation should be expected providing that the ratios $x_1/c \ll 1$, $y_1/2c \ll 1$ are satisfied.

Let the y_1 switching line be taken as a reference and assume that the system has been driven to the desired periodic behavior; that is, k = 1. An expression for the error in the desired quadrature phase relationship between the relay outputs f(x) and f(y) can be obtained in the following manner. The time elapsing from instant of y relay switching to x relay switching can be obtained by solving the equation of the x(t) motion

$$-x_1 = -c + e^{-(t - t_0)a}\,(x_\theta + c)$$

for $t - t_0$. Substituting for x_0 as given by equation (16) into the expression leads to

$$t - t_0 = \frac{1}{a}\,\ell n\,\frac{c\left(1 + \tanh\frac{a\,T_I}{4}\right)}{c - x_1} = \frac{T_I}{4} - \frac{1}{a}\,\ell n\left[(1 - x_1/c)\,\cosh\frac{a\,T_I}{4}\right]. \qquad (33)$$

If the output wave shapes have quadrature phase relationship, then the x relay must change polarity exactly $T_I/4$ seconds after the y relay. The last term of equation (33) therefore furnishes the deviation from the desired phase relationship as

$$\Delta\phi = \frac{2\pi}{a\,T_I}\,\ell n\left[(1 - x_1/c)\,\cosh\frac{a\,T_I}{4}\right]\ \text{(radians)}. \qquad (34)$$

SECTION VI. MECHANIZATION OF THE LOCK-ON OSCILLATOR

The lock-on oscillator circuit shown in Figure 11 was developed by H. Daniels, H. Farrow, and H. Hosenthien of the Flight Dynamics Branch, Astrionics Laboratory. It was found that the circuit possessed not only good lock-on characteristics over the expected frequency range, but also produced symmetrical output square waves with a relatively small inherent error in the quadrature phase relationship. A test case was run to present a comparison between experimental results and the corresponding theoretical results obtained through equations derived in the preceding analysis. The circuit values used were those shown in Figure 11; in particular, with a 5 μF input capacitor to the two relay sections. Table I presents a comparison of the theoretical and measured results for the conditions of free-run (no input) and with input signal (I(t)) frequencies of 0.7, 1.0, and 1.4 Hz.

TABLE 1. COMPARISON OF THEORETICAL AND MEASURED RESULTS FOR THE LOCK-ON OSCILLATOR CIRCUIT OF FIGURE 7

CASE	CONDITION	PREDICTED $f_{f.r.}$ (Hz)	PREDICTED $\Delta\phi$ (deg)	MEASURED $f_{f.r.}$ (Hz)	MEASURED $\Delta\phi$ (deg)
C = 5μF	Free-Run	1.39 Hz	0	1.31 Hz	0
C = 5μF	f_I = .7Hz		9.04		8.9
C = 5μF	f_I = 1.0Hz		4.12		2.0
C = 5μF	f_I = 1.4Hz		.07		1.3

A few comments are necessary with regard to the circuit. The relays were not subjected to direct analysis to obtain nonlinear characteristics, but were treated as "black boxes" and obtained experimentally. Figure 12 shows the x relay characteristic taken from an oscilloscope display when the circuit was in the free-run condition. As can be seen, the actual characteristic is very nearly that of the idealized case assumed in the preceding development of the equations. In the free-run conditions, account must be taken of the RC integrating networks on the form of the derived equations; however, the situation is otherwise unchanged from that assumed previously.

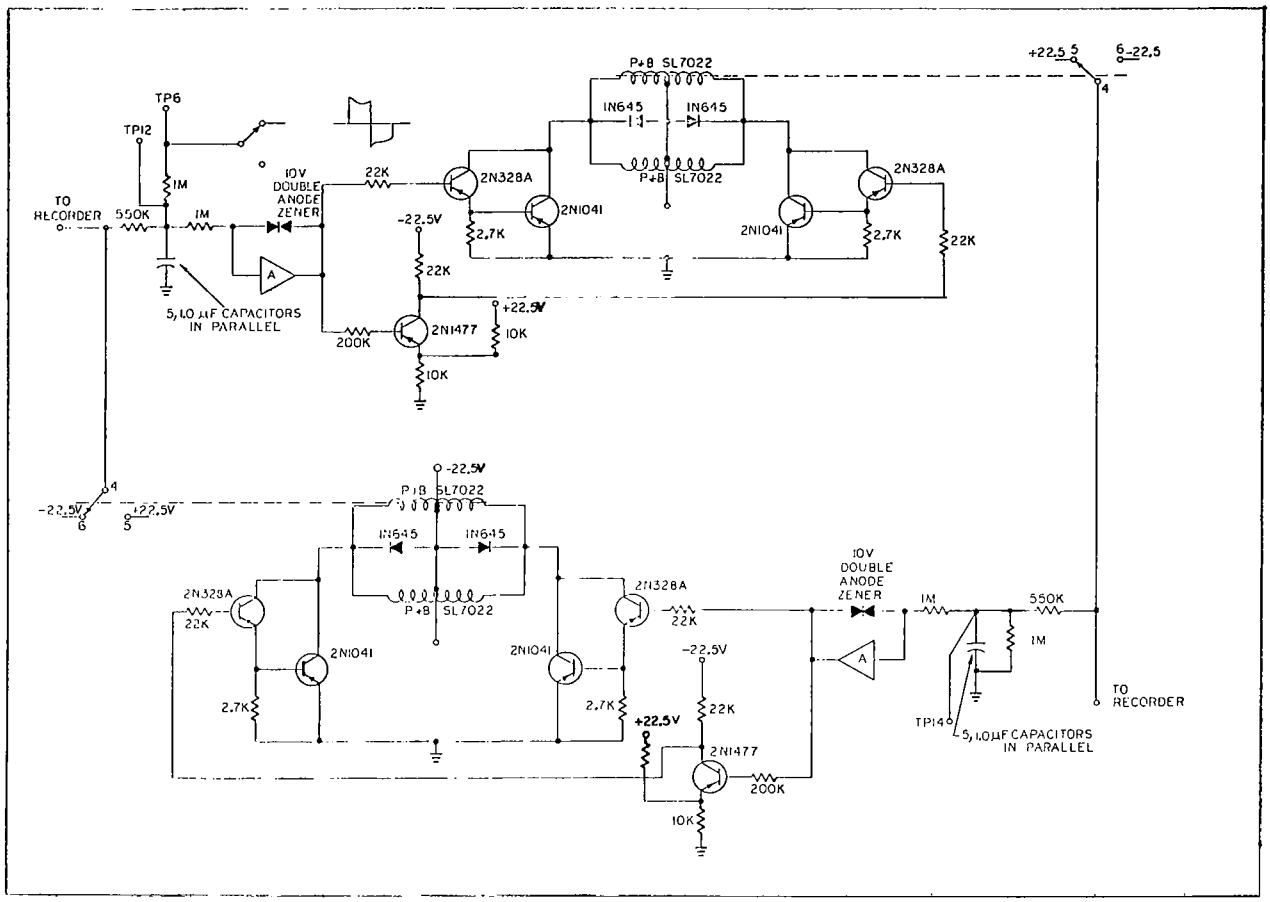

FIGURE 11. LOCK-ON OSCILLATOR CIRCUIT DIAGRAM

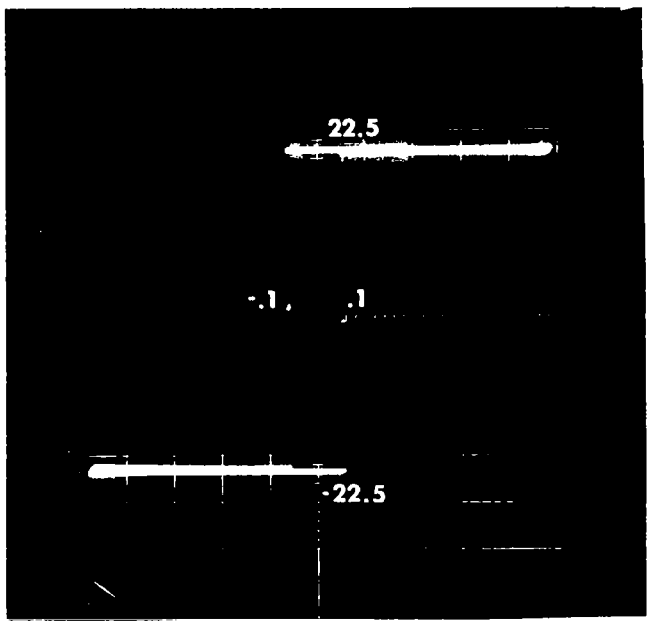

FIGURE 12. X RELAY CHARACTERISTIC

The following parameters are obtained from the circuit diagram of Figure 11:

$a = .7636$

$c = 10.714.$

Switching levels were obtained as

$x_1 = y_1 = .1.$

According to equation (11), the period of the free-running limit cycle is given by

$$T_{f.r.} = \frac{4}{a} \ell n \left[\frac{c + \sqrt{c(x_1 + y_1) - x_1 y_1}}{c - x_1} \right] = .72s \ .$$

The intersection of the free-run trajectory with the y_1 switching line is given by

$x_0 = \sqrt{c(x_1 + y_1) - x_1 y_1} = 1.46.$

Figure 13 illustrates the system in the free-running condition.

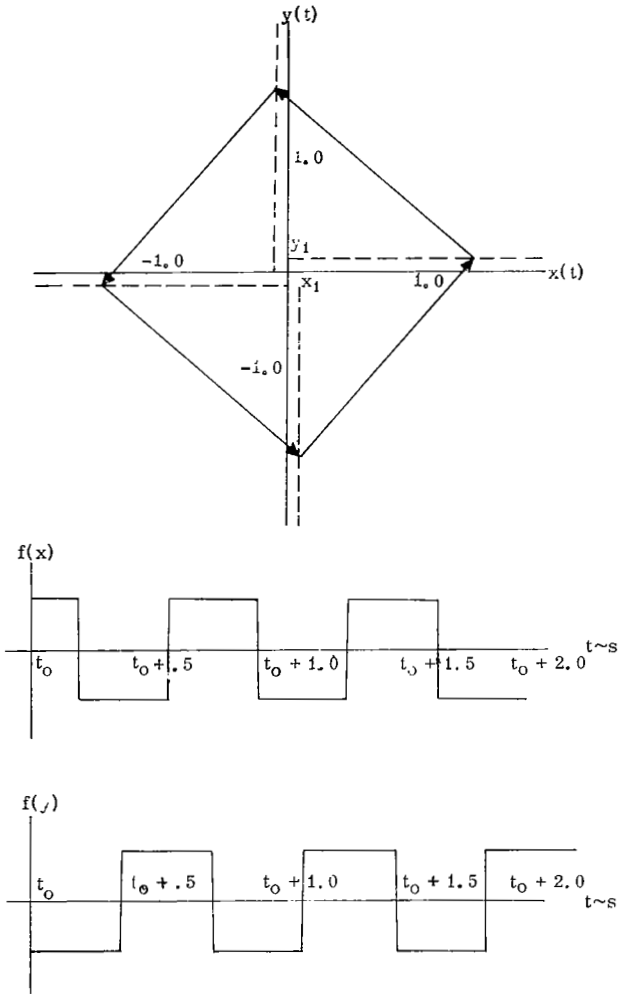

FIGURE 13. PREDICTED FREE-RUN TRAJECTORY AND RELAY OUTPUTS, C = 5 μF

Now consider the effect of applying an input I(t) with period T_I = 1.0 seconds. Equation (16) supplies the value x(t) must have at the instant of y relay switching to maintain the periodic trajectory, corresponding to k = 1, as

$$x(t_0) = c \tanh \frac{a\,T_I}{4} = 2.02 \ .$$

The error in the quadrature phase relationship is given by equation (34) as

$$\Delta\phi = \frac{360}{a\,T_I} \ln\left((1 - x_1/c)\cosh\frac{a\,T_I}{4}\right) = 4.12°.$$

Figure 14 shows the k = 1 trajectory and the corresponding input and output wave shapes. Figures 15 and 16 are further examples, illustrating the driven condition for the highest and lowest expected operating frequencies.

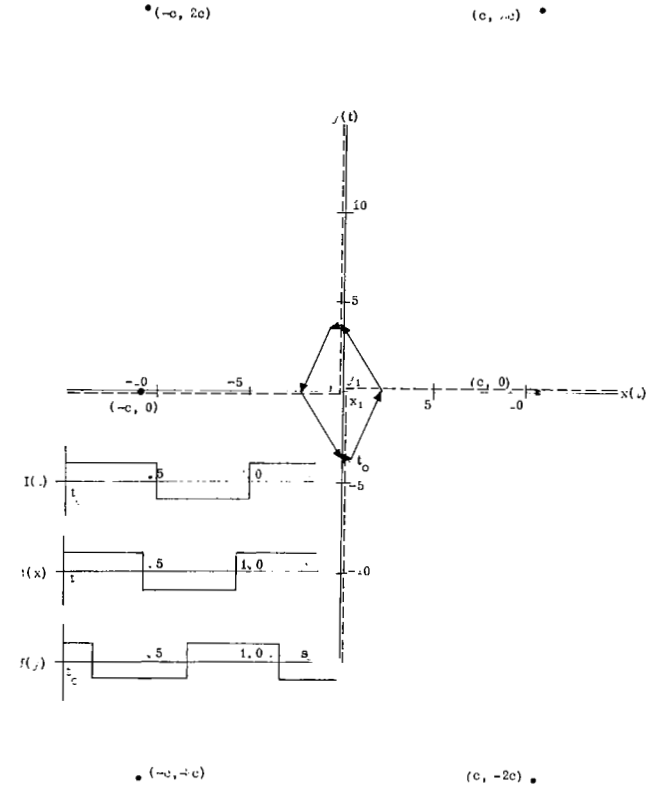

FIGURE 14. PREDICTED DRIVEN CONDITION FOR T_I = 1.0 SECOND, C = 5 μF

To determine whether trajectories corresponding to values of k greater than unity can exist in the expected frequency range, let T_I = .7143 seconds in equation (21) to obtain

$$e^{a(t_1 - t_0)} = \frac{\left(1 - \frac{y_1}{2c}\right)\left(1 + e^{-3a/2T_I}\right) - \frac{c + x(t_5)}{c - x_1}}{e^{-a/2T_I}\left(1 - e^{-aT_I/2} + e^{-a\,T_I}\right)}$$

$$= 1.31 \ .$$

Since

$$t_1 - t_0 = .3602 > \frac{T_I}{2} = .36 \ ,$$

higher ordered periodic trajectories should not exist. They will exist, however, for only slightly higher frequencies, as illustrated by Figure 17. The period of the driving signal of that example was obtained through use of equation (25).

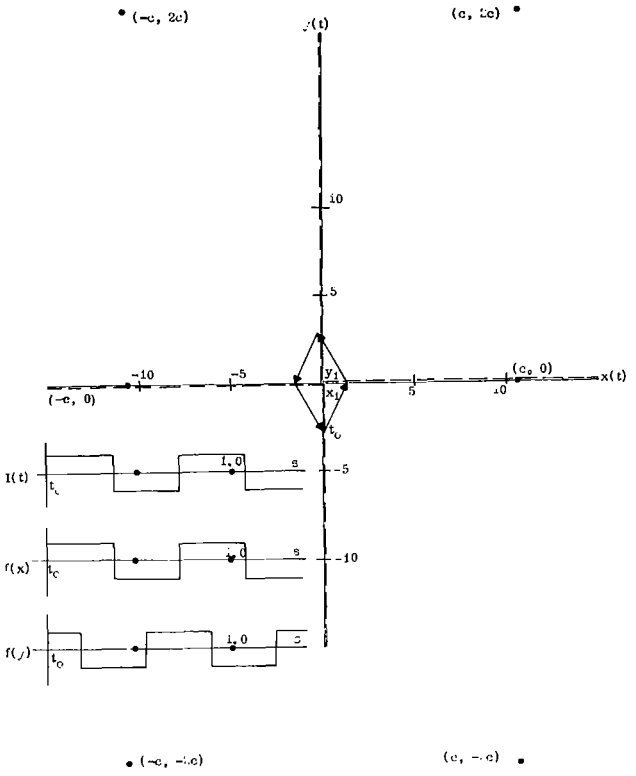

FIGURE 15. PREDICTED DRIVEN CONDITION FOR T_I = 0.7143 SECOND, C = 5 μF

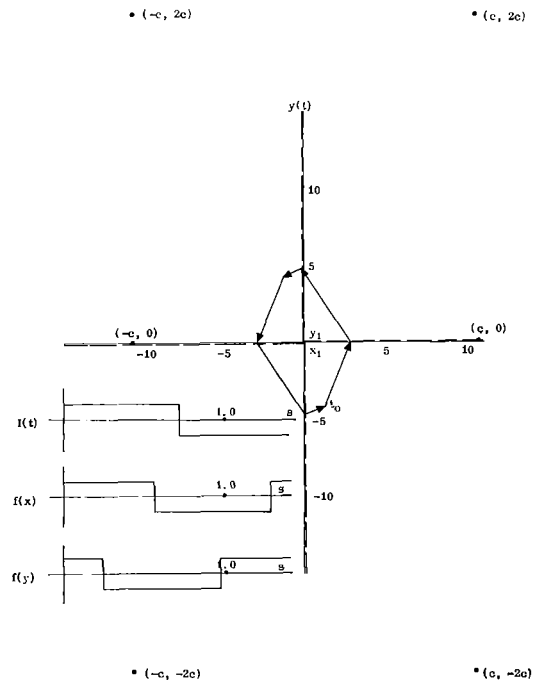

FIGURE 16. PREDICTED DRIVEN CONDITION FOR T_I = 1.43 SECOND, C = 5 μF

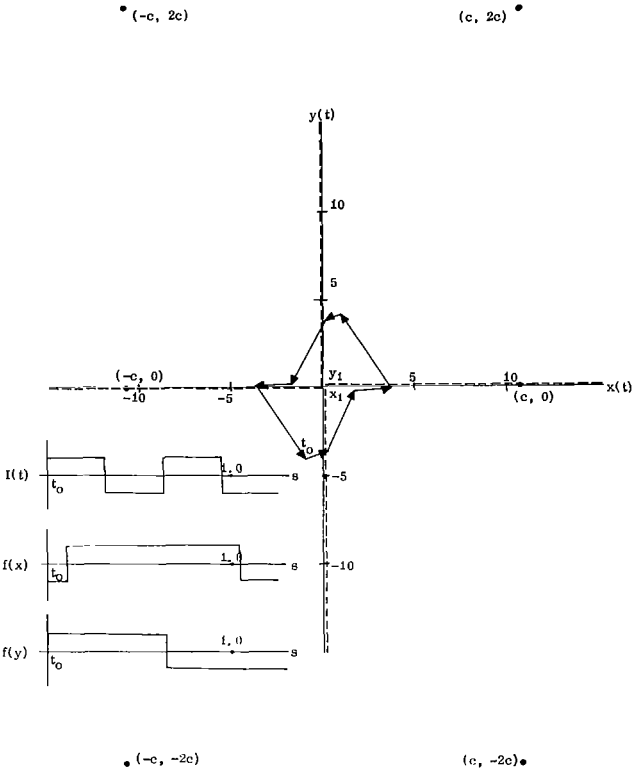

FIGURE 17. PREDICTED DRIVEN CONDITION FOR T_I = 0.63 SECOND, C = 5 μF, k = 3

Figures 18 through 22 are recordings made during operation of the circuit of Figure 11 and correspond to the predicted cases of Figures 13 through 17. Note particularly the k = 3 subharmonic lock-on case of Figures 17 and 22.

SECTION VII. CONCLUSION

The preceding analysis utilized phase space techniques to investigate the behavior of the lock-on oscillator in both the free-running and driven conditions. For the free-running condition, it was shown that a stable limit cycle exists and an expression obtained which permits prediction of the free-running frequency. In the driven case, the phase space technique permits determination of the existence of a periodic trajectory describing satisfactory tracking of the input signal frequency. From the form of such a trajectory, it was then possible to obtain an expression for the error in quadrature phase relationship between the two relay outputs. In addition to the existence of periodic trajectories indicating satisfactory tracking behavior, the phase plane approach indicated the existence of additional periodic trajectories which describe

a subharmonic tracking behavior. It was shown that the existence of such operating modes occurs at relatively low values of driving signal frequency, but with a suitable choice of parameters can be avoided through the frequency range expected for the particular application discussed in this report.

The analysis and results must be modified if the assumptions on equivalent relay outputs and input signal magnitudes are not valid. However, the techniques used should permit derivation of the corresponding results. This comment is equally applicable to the assumption on equivalent integrating network time constants and relay switching levels.

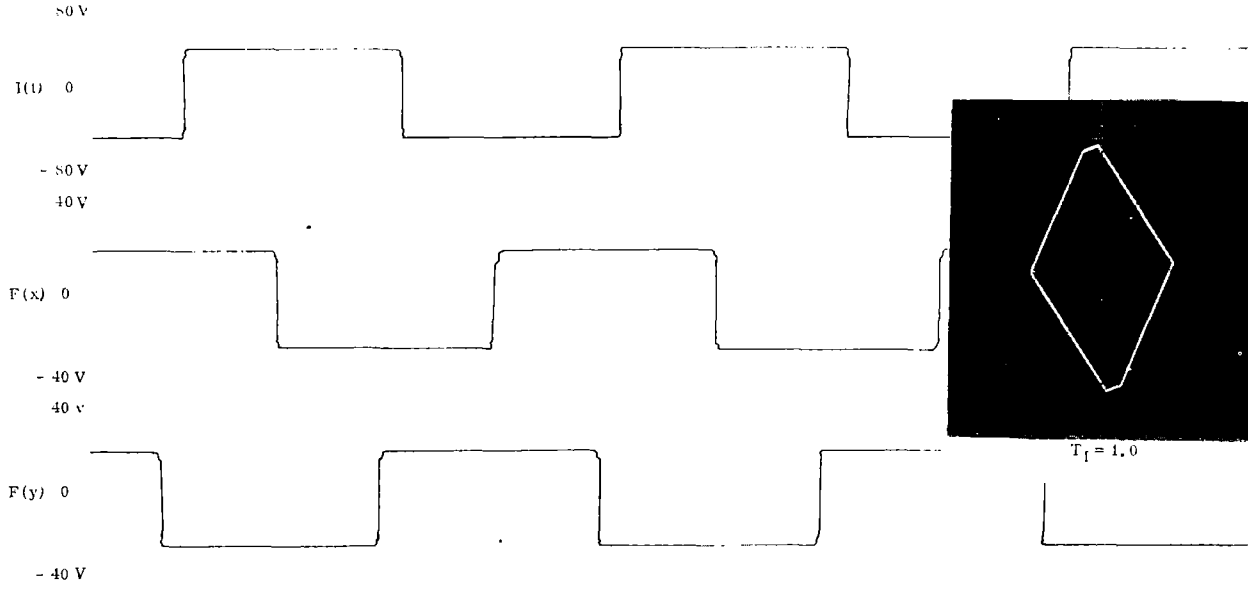

FIGURE 18. EXPERIMENTAL RESULTS, $T_I = 1.0$ SECOND

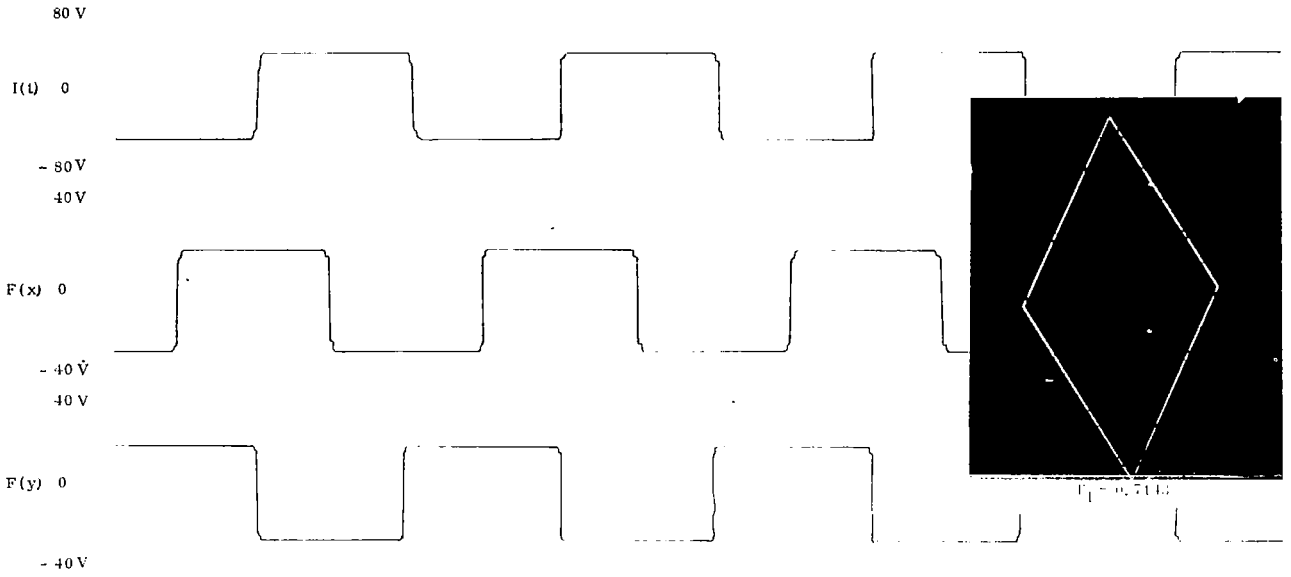

FIGURE 19. EXPERIMENTAL RESULTS, T_I = 0.7143 SECOND

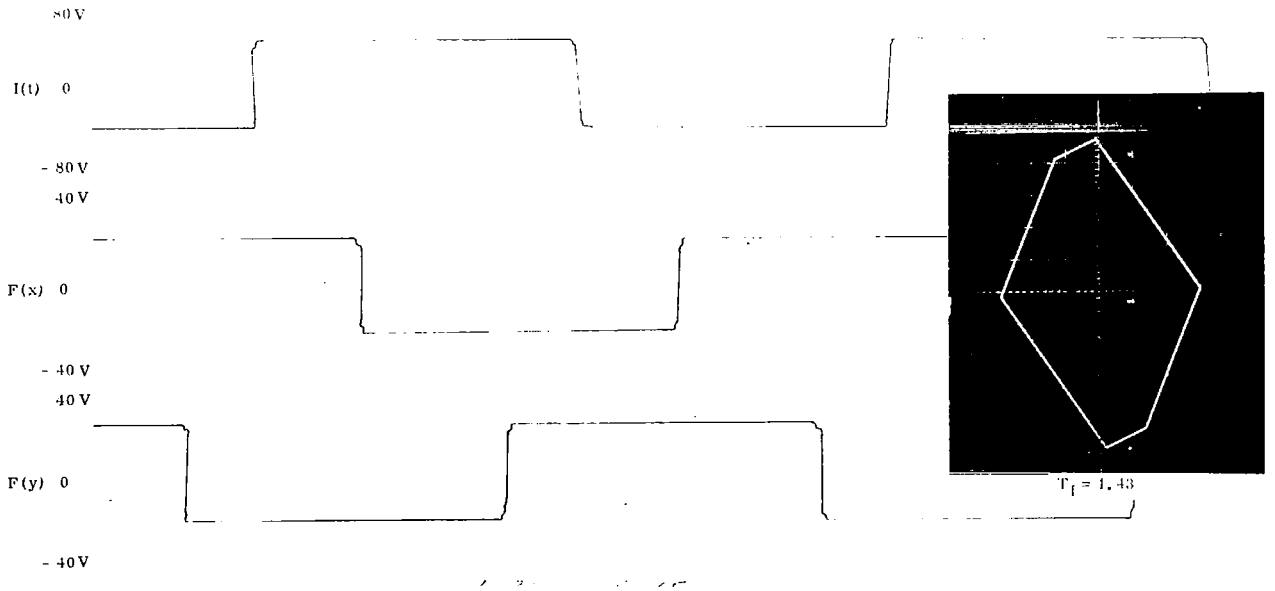

FIGURE 20. EXPERIMENTAL RESULTS, T_I = 1.43 SECOND

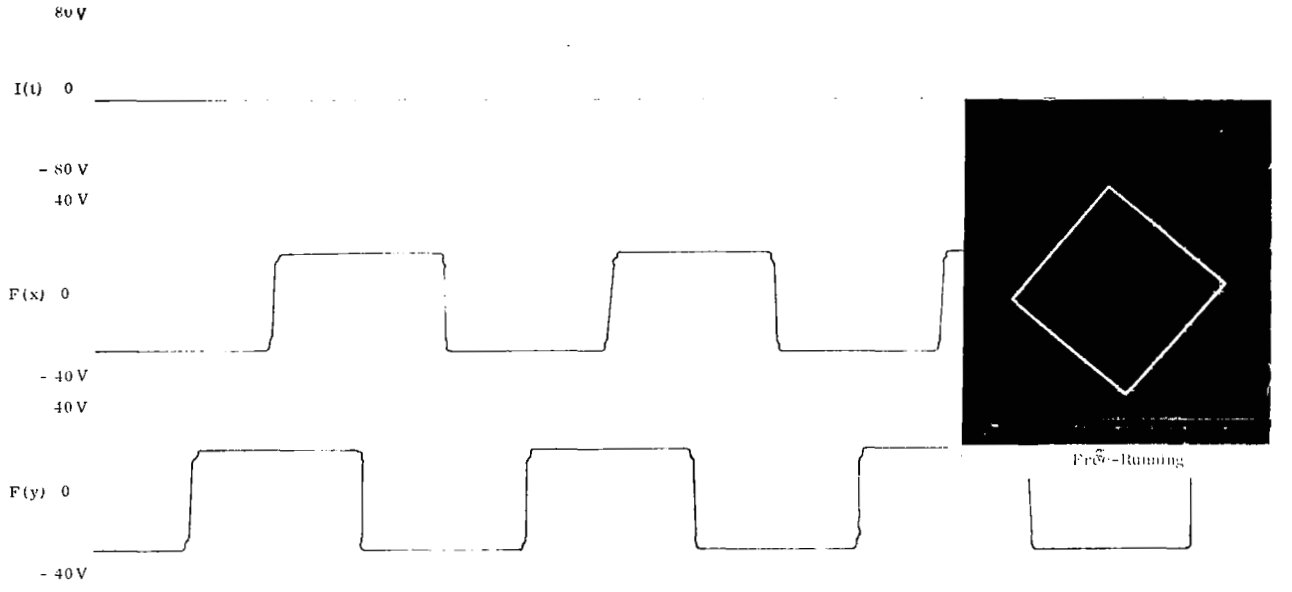

FIGURE 21. EXPERIMENTAL RESULTS, FREE-RUNNING

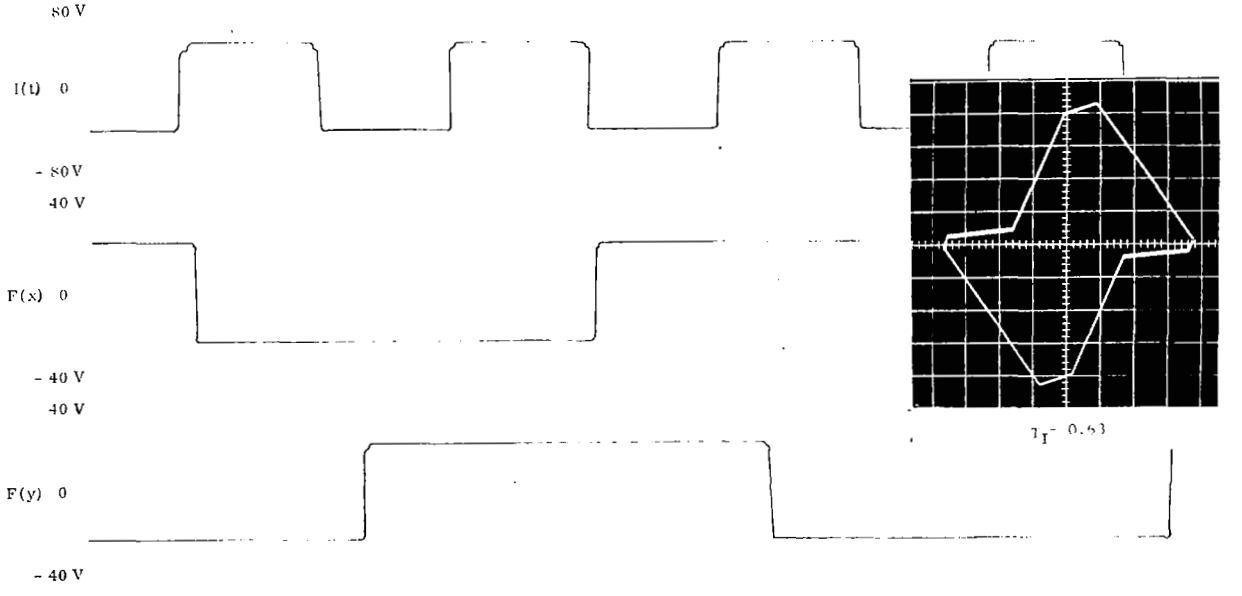

FIGURE 22. EXPERIMENTAL RESULTS, k = 3, FOR T_I = 0.63 SECOND

REFERENCES

1. Hosenthien, Hans H., and Borelli, Michael T.,"An Adaptive Tracking-Notch Filter for Suppression of Structural Bending Signals of Large Space Vehicles," Astrionics Research and Development Report No. 1, NASA TM X-53,000, October 1, 1963.
2. Terrazas, Carlos, and Fannin, Bill B., "Simulating Discontinuous Nonlinear Functions," Electronic Industries, August 1962, pp. 97-99.